AIAA JOURNAL
Vol. 44, No. 1, January 2006

Laminar Subsonic, Supersonic, and Transonic Boundary-Layer Flow past a Flat Plate

S. P. Otta* and A. P. Rothmayer†
Iowa State University, Ames, Iowa 50011

A boundary-layer formulation is developed for the low-Mach-number limit. Self-similar low-Mach-number Falkner–Skan solutions are found for flow past a wedge. From computation of both this low-Mach-number-limit solution and the full compressible boundary-layer equations, it is shown that laminar transonic boundary-layer flow past a constant temperature flat plate may be accurately calculated using the simpler low-Mach-number-limit solution.

Nomenclature

C	=	viscosity–density parameter
C_f	=	skin-friction coefficient
C_H	=	heat transfer coefficient
e, h	=	temperatures with and without Mach number heating
J	=	total enthalpy
M_∞	=	freestream Mach number
m_∞	=	parameter relating τ and M_∞
Pr	=	Prandtl number
Re	=	Reynolds number
T_c	=	temperature within the boundary layer scaled using $\lvert T_e - T_w \rvert$ for a flat plate
T_e, J_e	=	temperature and total enthalpy at the edge of the boundary layer
T_e^*	=	dimensional temperature at the edge of the boundary layer
T_w	=	nondimensional wall temperature
$\hat{T}$, $\hat{R}$	=	nondimensional perturbation temperature and density within the boundary layer
U, V	=	streamwise and wall-normal velocities
U_e	=	velocity at the edge of the boundary layer
β	=	pressure gradient parameter
ΔT^*	=	dimensional temperature difference between the freestream and the wall
ρ	=	density within the boundary layer
ρ_e, μ_e	=	density and viscosity at the edge of the boundary layer
ρ_w	=	nondimensional wall density
τ	=	freestream air temperature perturbation from wall temperature
$\psi, \Psi, \hat{\Psi}, f$	=	stream functions

Subscripts

e	=	property at the edge of the boundary layer
s, N	=	derivatives in boundary-layer equations
w	=	property at the wall
ξ, η	=	derivatives in boundary-layer equations in transformed coordinates

Superscript

$*$	=	dimensional quantity

Received 18 February 2005; revision received 18 August 2005; accepted for publication 18 August 2005.

*Graduate Assistant, Department of Aerospace Engineering and Engineering Mechanics. Student Member AIAA.

†Professor, Department of Aerospace Engineering and Engineering Mechanics. Associate Fellow AIAA.

I. Introduction

COMPRESSIBLE boundary layers have been extensively studied for a variety of applications from flat plates to swept wings and for subsonic Mach numbers to hypersonic Mach numbers. For low subsonic Mach numbers, it is often possible to assume incompressible flow. Hypersonic boundary layers at high Mach numbers generally involve strong interaction and strong viscous dissipation in a high-temperature, chemically reacting flow and require a more detailed set of equations. For transonic and supersonic flows, however, the boundary-layer equations are reasonably accurate, though changes in viscosity and thermal conductivity within the boundary layer must be taken into account.

In previous computations by other authors, the compressible boundary-layer equations have been solved with a variety of approximations. The viscosity–density parameter $\rho\mu/\rho_e\mu_e$ appearing in the transformed boundary-layer equations is computed using Sutherland's law, the power law, or a linear law. In some studies, the coefficient of proportionality for the linear law or the exponent in power law is such that the parameter $\rho\mu/\rho_e\mu_e$ is approximately constant, where e is the edge conditions in the boundary layer.[1–4] In addition, using a range of values of the exponent ω in the power law[5] or Sutherland's law (Van Driest[6]) allows this parameter to vary within the boundary layer (see also Refs. 7–11). More recently, Moraes et al.[12] (see also Ref. 13) gave a complete solution of the boundary-layer equations, while incorporating change of viscosity using Sutherland's law. In the current study, as in Refs. 6 and 12, Sutherland's law for viscosity is used along with the ideal gas assumption. In this study, the boundary-layer equations are solved, fully accounting for the change of viscosity and thermal conductivity within the boundary layer. The exact solution obtained from this computation is used for a comparison with simpler subsonic low Mach number solutions.

In contrast to solving the full compressible boundary layer equations, it is possible to use an asymptotic approach to simplify the equations. It has been studied by Herwig[14] and Gersten and Herwig.[15] As mentioned by Schlichting,[16] this approach uses a Taylor series expansion of properties such as density at the freestream temperature. The zero-order solution for this approach is the constant property incompressible boundary layer. The higher-order solution includes the effect of changes in Prandtl number and Eckert number. The Eckert number $Ec = U^{*2}/(c_p^* T^*)$ reduces to $(\gamma - 1)M_\infty^2$ for ideal gases. Additionally, Herwig[17] gave solutions for wedge flows using an asymptotic approach with two perturbation parameters, the first being the Eckert number and the second a heat transfer parameter. The heat transfer parameter is $\varepsilon = (T_w^* - T^*)/T^*$ for constant T_w^*.

In the current study, an alternate asymptotic formulation is developed for the boundary-layer equations at low subsonic Mach

numbers for aircraft icing where the wall is assumed to be at a constant freezing temperature for water.[18] A perturbation parameter, the freestream air temperature perturbation τ, is introduced at low subsonic Mach numbers, where boundary-layer heating due to viscous dissipation is comparable to freestream heating/cooling. When this parameter is used for expansions of basic flow quantities, such as density and temperature, the boundary-layer equations are then reduced to incompressible boundary-layer equations for momentum at zero-order and higher-order equations for temperature. Both nonsimilar and self-similar boundary layer equations are given, along with self-similar Falkner–Skan solutions. Because this perturbation is related to Mach number due to the assumed relationship between boundary-layer heating and freestream heating/cooling, it is possible to include the effect of both perturbation parameters used by Herwig[17] in properties such as density. It is shown that this asymptotic formulation for low Mach number subsonic boundary layers yields accurate results for transonic compressible boundary-layer flow past a flat plate. Because the subsonic formulation is much simpler than obtaining transonic boundary-layer solutions by direct computation, it is suggested that this low Mach number formulation for the flat plate may be used as a simplified test case for computational fluid dynamics and flow stability analysis.

II. Boundary-Layer Equations

When starting from the dimensional Navier–Stokes equations, the boundary-layer equations are obtained using boundary-layer scalings, which are based on freestream Reynolds number. The resulting equations are usually expressed as a continuity equation, an x-momentum equation, and an energy equation. The energy equation may be expressed in terms of temperature or total enthalpy. The form involving the total enthalpy is used in the current study.

For the Prandtl boundary layer, the momentum equation is[16]

$$\rho(UU_s + VU_N) = \rho_e U_e U_e'(s) + (\mu U_N)_N$$

The energy equation in total enthalpy form is given by

$$\rho(UJ_s + VJ_N) = \left[\mu(1 - 1/Pr)(U^2/2)_N\right]_N + [(\mu/Pr)J_N]_N$$

where s is the arclength along the surface, $n = Re^{-1/2}N$ is the boundary-layer coordinate normal to the surface, ρ is the density, and U and V are the streamwise and wall-normal velocities, respectively, within the boundary layer. The total enthalpy is expressed in terms of the temperature and velocity as follows:

$$J = \frac{1}{(\gamma - 1)M_\infty^2}T + \frac{1}{2}U^2$$

The boundary-layer equations are transformed into the Levy[3]–Lees[19] variables (also referred to as the Lees–Dorodnitsyn transformation; also see Illingworth,[20] Stewartson,[21] Howarth,[22] Dorodnitsyn,[23] and Anderson[24])

$$\xi = \int_0^s \rho_e \mu_e U_e \, \mathrm{d}s, \qquad \eta = \frac{U_e}{\sqrt{2\xi}} \int_0^N \rho \, \mathrm{d}N$$

When a stream function $\psi = \sqrt{(2\xi)}\, f(\xi, \eta)$ similar to the Görtler variables in incompressible boundary layers (see Ref. 16) is used, the ratios of the streamwise velocity and the total enthalpy within the boundary layer to the same quantities at the edge of the boundary layer may be expressed as

$$f_\eta(\xi, \eta) = U/U_e, \qquad g(\xi, \eta) = J/J_e$$

Because the total enthalpy is constant everywhere outside the boundary layer, and both the velocity and the temperature may be taken as unity in the freestream, the total enthalpy at the edge of the boundary layer may be written as

$$J_e = \frac{1}{(\gamma - 1)M_\infty^2} + \frac{1}{2}$$

The boundary-layer equations written in the Levy–Lees variables then become (see Ref. 16)

$$[Cf_{\eta\eta}]_\eta + ff_{\eta\eta} + \beta\left[\rho_e/\rho - f_\eta^2\right] = 2\xi(f_\eta f_{\eta\xi} - f_{\eta\eta} f_\xi) \tag{1}$$

$$\left[(C/Pr)g_\eta + C\left(U_e^2/J_e\right)(1 - 1/Pr)f_\eta f_{\eta\eta}\right]_\eta + fg_\eta = 2\xi(f_\eta g_\xi - g_\eta f_\xi) \tag{2}$$

where

$$C = \frac{\rho\mu}{\rho_e\mu_e}, \qquad \beta = \frac{2\xi}{U_e}\frac{\mathrm{d}U_e}{\mathrm{d}\xi}$$

These equations are valid for subsonic, transonic, and supersonic Mach numbers. At the wall, a fixed temperature or a heat transfer rate may be specified. At the edge of the boundary layer, T_e and U_e vary along the arclength.

III. Low-Mach-Number Solutions

A self-similar Falkner–Skan solution of this problem may be found at low Mach numbers (see Rothmayer[18]). In this limit, the airflow is assumed to be a low Mach number flow ($M_\infty \ll 1$) at approximately constant temperature. This implies that the flow is incompressible at leading order. In addition, it is assumed that the Mach number heating is comparable with freestream temperature perturbation τ, that is,

$$M_\infty = m_\infty \tau^{\frac{1}{2}} \tag{3}$$

where the temperature at the wall is expressed as $T_w = T^*_{\text{wall}}/T_\infty = [1 + \Delta T^*/T^*_{\text{wall}}]^{-1}$ and the temperature perturbation is defined to be

$$\tau = \frac{\Delta T^*}{T^*_{\text{wall}}} = \frac{\left|T_\infty - T^*_{\text{wall}}\right|}{T^*_{\text{wall}}} = \frac{|1 - T_w|}{T_w} \tag{4}$$

Because the dimensional temperature change is small, the perturbation $\tau \ll 1$. A limit solution is sought as $\tau \to 0$. The edge temperature of the boundary layer is given in terms of the edge velocity of the boundary layer U_e by

$$T_e = 1 + [(\gamma - 1)/2]m_\infty^2\left(1 - U_e^2\right)\tau + \cdots$$

In this limit, the stream function expansion within the boundary layer is found to be

$$\psi \sim Re^{-\frac{1}{2}}\Psi + Re^{-\frac{1}{2}}\tau\hat{\Psi} + \cdots$$

and the density and temperature expansions are

$$(\rho, T) \sim (1, 1) + \tau(\hat{R}, \hat{T}) + \cdots \tag{5}$$

The resulting boundary-layer equations are

$$\Psi_N\Psi_{sN} - \Psi_s\Psi_{NN} = U_e U_e'(s) + \Psi_{NNN}$$

$$\Psi_N\hat{T}_s - \Psi_s\hat{T}_N = (\gamma - 1)m_\infty^2\left[-\Psi_N U_e U_e'(s) + \Psi_{NN}^2\right] + Pr^{-1}\hat{T}_{NN} \tag{6}$$

The preceding equations may be rewritten using Görtler variables,

$$\xi = \int_0^s U_e(s) \, \mathrm{d}s, \qquad \eta = \frac{U_e N}{\sqrt{2\xi}}, \qquad \Psi = \sqrt{2\xi}\, f(\xi, \eta)$$

in which case, the stream function equation reduces to

$$f_{\eta\eta\eta} + ff_{\eta\eta} + \beta\left[1 - f_\eta^2\right] = 2\xi[f_\eta f_{\xi\eta} - f_\xi f_{\eta\eta}] \tag{7}$$

with the following boundary conditions: $f(\xi, 0) = f_\eta(\xi, 0) = 0$ and $f_\eta(\xi, \infty) \to 1$. Likewise, the energy equation reduces to

$$(1/Pr)\hat{T}_{\eta\eta} + f\hat{T}_\eta + (\gamma - 1)m_\infty^2 U_e^2\left[f_{\eta\eta}^2 - \beta f_\eta\right] = 2\xi(f_\eta\hat{T}_\xi - \hat{T}_\eta f_\xi) \tag{8}$$

with the boundary conditions $\hat{T}(\xi, 0) = \mp 1$ and $\hat{T}(\xi, \infty) \to [(\gamma - 1)/2]m_\infty^2(1 - U_e^2)$. The upper/lower sign for the wall boundary condition refers to the freestream temperature above/below the wall temperature. The temperature field is decomposed into the zero-Mach-number solution and the contribution at higher subsonic Mach numbers, that is,

$$\hat{T} = \pm[e(\xi, \eta) - 1] + [(\gamma - 1)/2]m_\infty^2\left[e(\xi, \eta) - U_e^2 h(\xi, \eta)\right] \quad (9)$$

The energy equation is rewritten using the preceding linear decomposition for temperature and the two temperatures e and h satisfy

$$Pr^{-1}e_{\eta\eta} + fe_\eta = 2\xi[f_\eta e_\xi - f_\xi e_\eta] \quad (10)$$

with boundary conditions $e(\xi, 0) = 0$ and $e(\xi, \infty) = 1$ and

$$Pr^{-1}h_{\eta\eta} + fh_\eta - 2\beta f_\eta h = 2\left[f_{\eta\eta}^2 - \beta f_\eta\right] + 2\xi[f_\eta h_\xi - f_\xi h_\eta] \quad (11)$$

with boundary conditions $h(\xi, 0) = 0$ and $h(\xi, \infty) = 1$.

Self-similar Falkner–Skan solutions for the preceding equations may be obtained for flows past wedges, where the inviscid solution is $U_e = U_{e0}s^{\beta/(2-\beta)}$ and the boundary-layer coordinate and the stream function are

$$\eta = \sqrt{U_{e0}/(2-\beta)}Ns^{(\beta-1)/(2-\beta)}$$

$$\Psi = \sqrt{U_{e0}(2-\beta)}s^{1/(2-\beta)}f(\eta)$$

Here β is the standard pressure gradient parameter. The stream function satisfies the well-known Falkner–Skan equation

$$f_{\eta\eta\eta} + ff_{\eta\eta} + \beta\left[1 - f_\eta^2\right] = 0 \quad (12)$$

with $f(0) = f_\eta(0) = 0$ and $f_\eta(\infty) \to 1$. The temperature split [Eq. (9)] becomes

$$\hat{T} = \pm[e(\eta) - 1] + [(\gamma - 1)/2]m_\infty^2\left[e(\eta) - U_{e0}^2 s^{2\beta/(2-\beta)}h(\eta)\right]$$

The two functions e and h now satisfy

$$Pr^{-1}e_{\eta\eta} + fe_\eta = 0 \quad (13)$$

with boundary conditions $e(0) = 0$ and $e(\infty) = 1$ and

$$Pr^{-1}h_{\eta\eta} + fh_\eta - 2\beta f_\eta h = 2\left[f_{\eta\eta}^2 - \beta f_\eta\right] \quad (14)$$

with boundary conditions $h(0) = 0$ and $h(\infty) = 1$. The skin-friction and heat transfer coefficients for the self-similar solution are found to be

$$C_f = \lambda = U_N(s, 0) = U_{e0}\sqrt{U_{e0}/(2-\beta)}s^{(2\beta-1)/(2-\beta)}f_{\eta\eta}(0)$$

$$C_H = q_w = \hat{T}_N(s, 0) = \sqrt{U_{e0}/(2-\beta)}s^{(\beta-1)/(2-\beta)}$$

$$\times\left\{\pm e_\eta(0) + [(\gamma - 1)/2]m_\infty^2\left[e_\eta(0) - U_{e0}^2 s^{2\beta/(2-\beta)}h_\eta(0)\right]\right\} \quad (15)$$

The solutions of the Falkner–Skan equation and the energy equation are shown in Figs. 1–5. The skin friction is compared with the results from White[25] and Davis et al.[26] A grid size study is shown in Figs. 1, 3, and 5. Figures 1, 3, and 5 show both a coarse and fine grid solution. The Prandtl number is taken to be 0.72, and β is taken to be approximately 1.0, 0.0, and −0.1989 for the upper branch and −0.1, −0.05, and −0.01 for the lower branch. As β decreases from 1 to −0.1989 on the upper branch, the boundary-layer thickness increases. On the lower branch, part of the boundary layer is separated. The separated region grows as $\beta \to 0$. Both the temperatures e and h show an increase in the thermal boundary layer thickness as the flow becomes more separated (Figs. 2 and 4), accompanied by a decrease in the heat flux at the wall at fixed Mach number (Figs. 3 and 5). Adverse pressure gradients affect the temperature h more strongly than the temperature e, as seen in the sharp increase for the temperature h near the wall (Fig. 4). Note that the heat flux at the wall for the temperatures e and h is positive for all β and the heat flux approaches 0 as $\beta \to 0$ along the lower branch for the fully separated boundary layer.

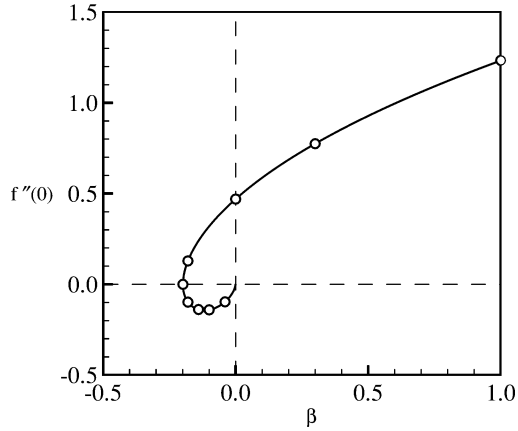

Fig. 1 Wall skin-friction parameter with $Pr = 0.72$: ——, coarse- and fine-grid solutions and ○, data from White[25] for upper branch and Davis et al.[26] for lower branch.

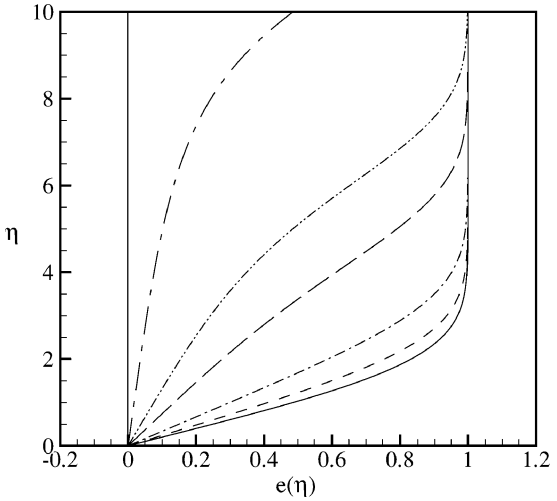

Fig. 2 Self-similar temperature function e with $Pr = 0.72$: ——, $\beta = 1.0$; – – –, 0.0; –·–, −0.1989; ——, −0.1; –··–, −0.05; and ——·——, −0.01.

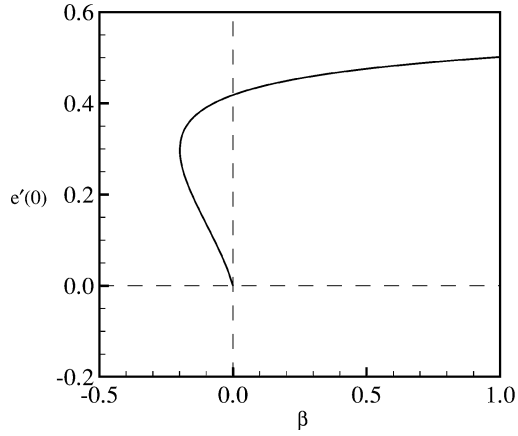

Fig. 3 Wall heat flux parameter of self-similar temperature function e with $Pr = 0.72$: both coarse- and fine-grid solutions.

IV. Validation Using High-Mach-Number Solutions

Numerical solutions are found for the following finite-Mach-number self-similar boundary-layer equations for flow past a flat plate:

$$[Cf_{\eta\eta}]_\eta + ff_{\eta\eta} + \beta\left[\rho_e/\rho - f_\eta^2\right] = 0 \quad (16)$$

$$\left[(C/Pr)g_\eta + C\left(U_e^2/J_e\right)(1 - 1/Pr)f_\eta f_{\eta\eta}\right]_\eta + fg_\eta = 0 \quad (17)$$

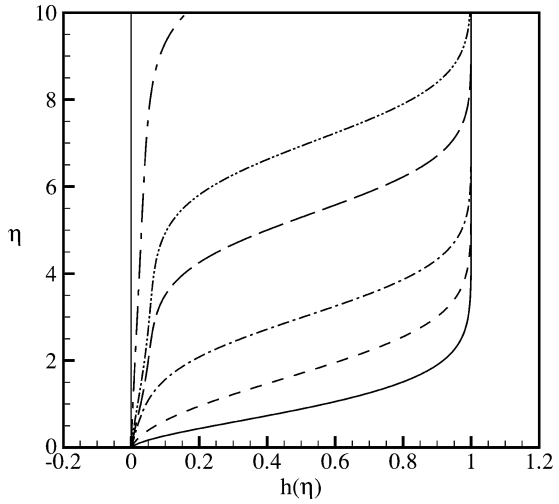

Fig. 4 Self-similar temperature function h with $Pr = 0.72$: ——, $\beta = 1.0$; – – –, 0.0; –·–, −0.1989; — —, −0.1; –··–, −0.05; and — · —, −0.01.

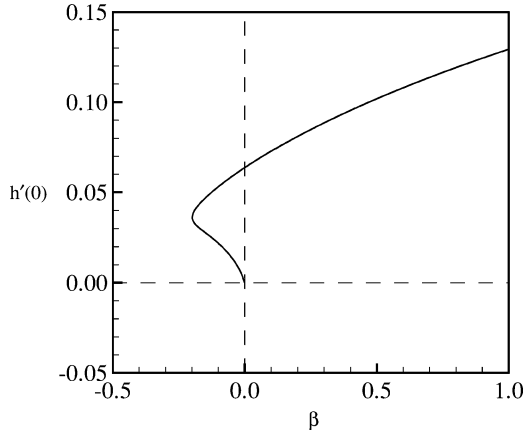

Fig. 5 Wall heat flux parameter of self-similar temperature function h with $Pr = 0.72$: both coarse- and fine-grid solutions.

Viscosity is calculated using Sutherland's law, and density is calculated from the relation $\rho_e T_e = \rho T$. This approach fully accounts for changes in viscosity and density within the boundary layer. For the flat plate, $U_e = 1$ and $T_e = 1$. J_e is constant for a given Mach number. A second-order-accurate Crank–Nicolson method is used to solve Eqs. (16) and (17) (Tannehill[27]; also see Ref. 28).

The edge temperature T_e and wall temperature T_w are taken to be fixed. The Prandtl number is taken to be 0.72, and the temperature T_c is given by

$$T_c = [T - T_w]/|T_e - T_w|$$

The effect of viscous heating within the boundary layer is evident in the temperature T_c. The velocity profile shows insignificant change with an increase in Mach number up to $M_\infty = 1.5$. The zero-Mach-number solution is taken from Eqs. (12–14) with $m_\infty = 0$.

To check the validity of the computations, a comparison is made with a case where $T_w = T_e$, $T_e^* = 217.67$ K and $Pr = 0.75$ (see Van Driest[6]). It is understood that the calculation being done for laminar compressible boundary layers does not account for the effects of turbulence or the viscous/inviscid hypersonic boundary-layer interactions at high Mach numbers. The primary objective of the comparison is to validate the numerical calculations.

To go from the Levy–Lees variables of Eqs. (1) and (2) to the physical coordinate, the inverse transformation

$$N = \left(\frac{\sqrt{2\xi}}{U_e}\right)\int_0^\eta \left(\frac{1}{\rho}\right) \mathrm{d}\eta$$

is used. For the flat plate, $\rho_e = 1$, $\mu_e = 1$, and $U_e = 1$, and this implies that

$$\xi = \int_0^s \rho_e \mu_e U_e \, \mathrm{d}s = s$$

Thus, the inverse transformation for the physical coordinates is[29]

$$s = \xi \qquad N = \sqrt{2\xi}\int_0^\eta \left(\frac{1}{\rho}\right) \mathrm{d}\eta$$

When these inverse transformations are used, the calculations for velocity and temperature are shown in physical coordinates at $s = 1$ (Figs. 6 and 7). It is seen that the results compare well with those of Van Driest.[6] The change of the viscosity–density parameter across the boundary layer is shown in Fig. 8. It may be observed here that the viscosity–density parameter does not change more than 10% for the lower Mach numbers. Thus, in Eqs. (1) and (2), the viscosity–density parameter C may be assumed to be equal to 1. Figure 9 shows that for Mach number equal to 4.0 the differences in the temperatures profiles are not significant. For Mach number equal to 8.0, these differences are significant. A similar behavior occurs for velocity. This implies that for cases corresponding to higher Mach numbers the viscosity–density parameter C should be included in the calculations.

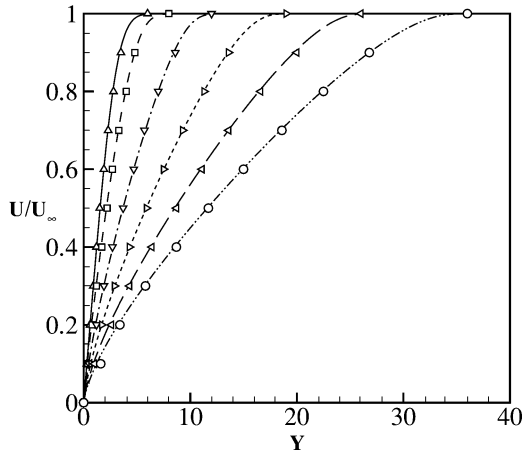

Fig. 6 Velocity in physical coordinates with $T_w = T_e$, $T_e^* = 217.67$ K, $Pr = 0.75$ at $s = 1$: ——, $M_\infty = 0.0$; – – –, 4.0; –·–, 8.0; - - - -, 12.0; — —, 16.0; –··–, 20.0; and for Van Driest's[6] case: △, $M_\infty = 0.0$; □, 4.0; ▽, 8.0; ▷, 12.0; ◁, 16.0; and ○, 20.0.

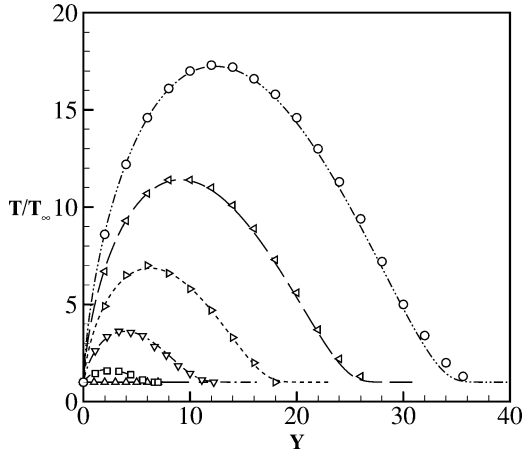

Fig. 7 Temperature in physical coordinates with $T_w = T_e$, $T_e^* = 217.67$ K, $Pr = 0.75$ at $s = 1$: ——, $M_\infty = 0.0$; – – –, 4.0; –·–, 8.0; - - - -, 12.0; — —, 16.0; –··–, 20.0 and for Van Driest's case: △, $M_\infty = 0.0$; □, 4.0; ▽, 8.0; ▷, 12.0; ◁, 16.0; and ○, 20.0.

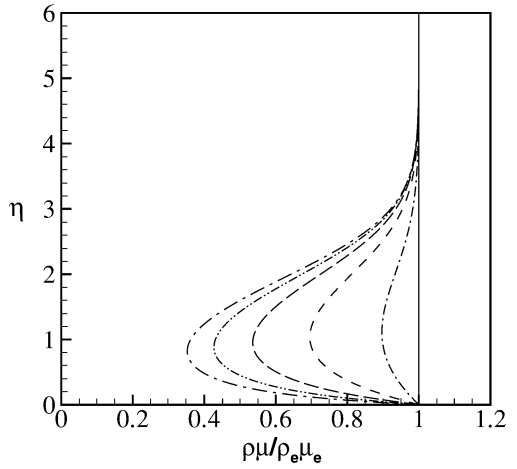

Fig. 8 Variation of viscosity-density parameter with $T_w = T_e$, $T_e^* = 217.67$ K, $Pr = 0.75$ at $s = 1$: ——, $M_\infty = 0.0$; –·–, 4.0; – – –, 8.0; ——, 12.0; –··–, 16.0; and —·—, 20.0.

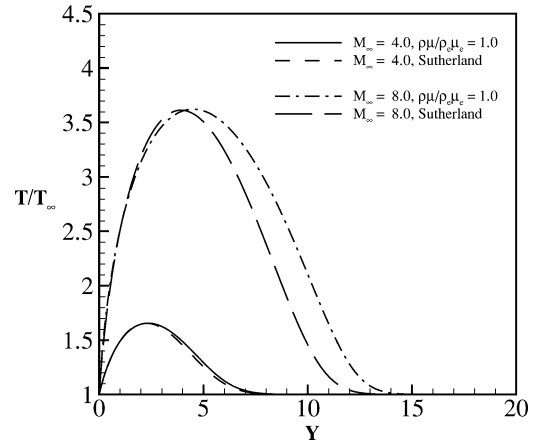

Fig. 9 Temperature for constant and varying viscosity-density parameter with $T_w = T_e$, $T_e^* = 217.67$ K, $Pr = 0.75$ at $s = 1$.

V. Comparison with Low-Mach-Number Solutions

A comparison is made between the finite-Mach-number transonic boundary-layer calculations and the low-Mach-number asymptotic equations for $\tau \ll 1$. The formal connection between the two solutions may be shown using the expression for the temperature inside the boundary layer [Eq. (5)] and the relationship between the Mach number and the temperature perturbation [Eq. (3)]. The ratio of the total enthalpy to the total enthalpy at the edge of the boundary layer then reduces to

$$g = 1 + \tau \hat{g} + \cdots$$

where $\hat{g} = [\hat{T} - \frac{1}{2}(\gamma - 1)m_\infty^2(1 - U_e^2 f_\eta^2)]$. When this expansion is used, the energy equation (2) for the nonsimilar compressible boundary layer becomes

$$[(1/Pr)\hat{T}_\eta]_\eta + f\hat{T}_\eta + (\gamma - 1)m_\infty^2 U_e^2\left[f_{\eta\eta}^2 - \beta f_\eta\right] = 2\xi(f_\eta \hat{T}_\xi - \hat{T}_\eta f_\xi) \tag{18}$$

Equation (18) is identical to the transformed temperature perturbation equation (8) derived from Eq. (6) when the Prandtl number is constant. When the temperature decomposition for the nonsimilar boundary layer [Eq. (9)] is used, this equation reduces to Eqs. (10) and (11) and ultimately to Eqs. (13) and (14), when using a self-similar approximation.

The heat transfer coefficient at the wall for the finite Mach number self-similar problem may be written as follows:

$$C_H = q_w = \sqrt{\frac{1}{2s}}\rho_w \frac{\partial T_c}{\partial \eta}(0) \tag{19}$$

The results computed for the transonic boundary layer are compared to the heat transfer coefficient computed from the low-Mach-number self-similar solution (15), which takes the following form for flow past a flat plate:

$$C_H = q_w = \hat{T}_N(s, 0) = \sqrt{1/2s}\left\{\pm e_\eta(0) + [(\gamma - 1)/2] \times m_\infty^2[e_\eta(0) - h_\eta(0)]\right\} \tag{20}$$

The comparisons of the heat transfer coefficients [plotted as $\sqrt{(2s)}C_H$] are shown in Figs. 10 and 11. The actual heat transfer coefficient is obtained by multiplying Eq. (19) with $|T_e - T_w|$. The dimensional wall temperature is fixed at 273.15 K. The dimensional temperature at the edge of the boundary layer is expressed in terms of the wall temperature and a dimensional temperature difference ΔT^*, as $T_e^* = T_\infty = T_{\text{wall}}^* - \Delta T^*$ for the flat plate. The air temperature perturbation τ is computed using the definition of Eq. (4). As the factor m_∞ increases, the Mach number [Eq. (3)] increases for a fixed air temperature perturbation. The heat transfer coefficient increases

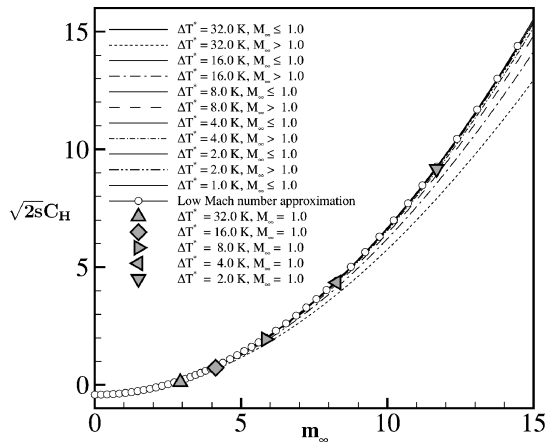

Fig. 10 Comparison of wall heat transfer of transonic calculations with low Mach number limit solution: darkened symbols, location of $M_\infty = 1$ point on computed transonic heat transfer curve for given dimensional temperature difference ΔT^* where $T_{\text{wall}}^* = 273.15$ K, $T_e^* = T_\infty = T_{\text{wall}}^* - \Delta T^*$.

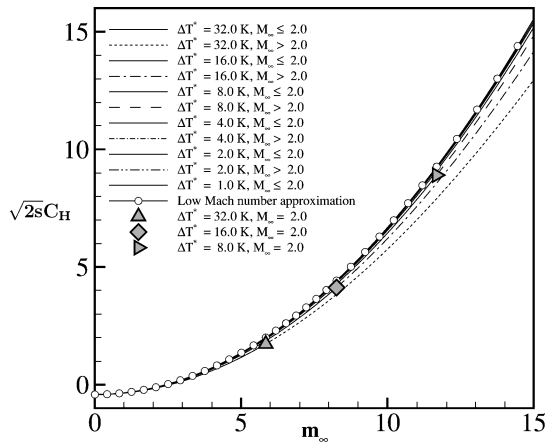

Fig. 11 Comparison of wall heat transfer of transonic calculations with low Mach number limit solution: darkened symbols, location of $M_\infty = 2$ point on computed transonic heat transfer curve for given dimensional temperature difference ΔT^* where $T_{\text{wall}}^* = 273.15$ K, $T_e^* = T_\infty = T_{\text{wall}}^* - \Delta T^*$.

along with the increase in Mach number. In Fig. 10, the heat transfer coefficient is shown with changing m_∞ and is divided into two regions, the first region with $M_\infty \leq 1$ and the second with $M_\infty > 1$. (The dividing Mach number at $M_\infty = 1$ is identified by a darkened symbol.) In all cases, it may be seen that the darkened symbol at $M_\infty = 1$ is very close to the low Mach number solution for heat transfer. Similarly, in Fig. 11, the curves for heat transfer coefficient are divided into different regions, the first region with $M_\infty \leq 2$ and the second with $M_\infty > 2$. (The dividing Mach number at $M_\infty = 2$ is identified by a darkened symbol.) When Figs. 10 and 11 are considered, it may be seen that the darkened symbols for the Mach numbers dividing the low- and high-Mach-number heat transfer curves are gradually moving away from the solution for low Mach numbers, as the Mach number increases. However, this change is small even at $M_\infty = 2$, and the heat transfer predicted from the low-Mach-number solutions may be used without much loss of accuracy. This is consistent with the observations of Herwig[17] that an asymptotic theory using perturbation parameters is valid at higher Mach numbers.

VI. Summary

The steady laminar boundary-layer equations are solved for subsonic, transonic, and supersonic flow past a flat plate, and the solutions are compared with the work of other authors. A simple self-similar low-Mach-number limit solution is obtained for Falker–Skan flows past wedges. Comparison of the low-Mach-number solution and the full boundary-layer computations reveal that the limit solution can accurately capture boundary-layer surface heat flux up through low supersonic Mach numbers.

Acknowledgments

This research was partially supported by the Icing Branch at the NASA John H. Glenn Research Center at Lewis Field, under Contract NAG-3-2863. The authors thank M. Potapczuk for his helpful guidance and support.

References

[1]Crocco, L., "Sulla strato limite laminaire nei gas lungo una lamina plana," *Rend. Mat. Univ. Roma*, Vol. 2, 1941, p. 138.

[2]Hantzsche, W., and Wendt, H., "Zum kompressibilitätseinfluß bei der lamiaren Grenzschicht der ebenen platte," *Jb. dt. Luftfahrtforschung I*, 1940, pp. 517–521.

[3]Levy, S., "Effect of Large Temperature Changes (Including Viscous Heating) upon Laminar Boundary Layers with Variable Free-Stream Velocity," *Journal of the Aeronautical Sciences*, Vol. 21, No. 7, 1954, pp. 459–474.

[4]Chapman, D. R., and Rubesin, M. W., "Temperature and Velocity Profiles in the Compressible Laminar Boundary Layer with Arbitrary Distribution of Surface Temperature," *Journal of the Aeronautical Sciences*, Vol. 16, No. 9, 1949, pp. 547–565.

[5]Dewey, C. F., Jr., and Gross, J. F., "Exact Similar Solutions of the Laminar Boundary-Layer Equations," *Advances in Heat Transfer*, Vol. 4, Oct. 1967, pp. 317–446.

[6]Van Driest, E. R., "Investigation of Laminar Boundary Layer in Compressible Fluids Using the Crocco Method," NACA TN-2597, Jan. 1952.

[7]Cohen, C. B., and Reshotko, E., "Similar Solutions for the Compressible Laminar Boundary Layer with Heat Transfer and Pressure Gradient," NACA TR-1293, Jan. 1956.

[8]Li, T. Y., and Nagamatsu, H. T., "Similar Solutions of Compressible Boundary Layer Equations," *Journal of the Aeronautical Sciences*, Vol. 22, No. 9, 1955, pp. 607–616.

[9]Back, L. H., and Cuffel, R. F., "Compressible Laminar Boundary Layers with Large Acceleration and Cooling," *AIAA Journal*, Vol. 14, No. 7, 1976, pp. 968–971.

[10]Kaups, K., and Cebeci, T., "Compressible Laminar Boundary Layers with Suction on Swept and Tapered Wings," *Journal of Aircraft*, Vol. 14, No. 7, 1977, pp. 661–667.

[11]Smith, A. M. O., and Clutter, D. W., "Machine Calculation of Compressible Laminar Boundary Layers," *Journal of Spacecraft and Rockets*, Vol. 40, No. 5, 2003, pp. 742–750 (1965 reprint).

[12]Moraes, A., Flaherty, J., and Nagamatsu, H. T., "Compressible Laminar Boundary Layers for Perfect and Real Gases in Equilibrium at Mach Numbers up to 30," AIAA Paper 92-0757, Jan. 1992.

[13]Toro, P. G. P., Rusak, Z., Nagamatsu, H. T., and Myrabo, L. N., "Self-Similar Compressible Laminar Boundary Layers," AIAA Paper 97-0767, Jan. 1997.

[14]Herwig, H., "Asymptotische Theorie zur Erfassung des Einflusses variabler Stoffwerte auf Impuls-und Wärmeübertragung," *Strömungstechnik*, Reihe 7, No. 93, Verein Deutscher Ingenieure.; Fortschritt-Berichte der VDI-Zeitschriften, VDI-Verlag, Düsseldorf, Germany, 1985, p. 212.

[15]Gersten, K., and Herwig, H., *Strömungsmechanik. Grundlagen de Impuls-, Wärme- und Stoffübertragung aus asymptotischer Sicht*, Vieweg-Verlag, Braunschweig, Germany, 1992.

[16]Schlichting, H., and Gersten, K., *Boundary Layer Theory*, Springer-Verlag, Berlin, 1999, pp. 241–257.

[17]Herwig, H., "An Asymptotic Approach to Compressible Boundary Layer Flow," *International Journal of Heat and Mass Transfer*, Vol. 30, No. 1, 1987, pp. 59–68.

[18]Rothmayer, A. P., "Scaling Laws for Water and Ice Layers on Airfoils," AIAA Paper 2003-1217, Jan. 2003.

[19]Lees, L., and Reshotko, E., "Stability of the Compressible Laminar Boundary Layer," *Journal of Fluid Mechanics*, Vol. 12, 1962, pp. 555–590.

[20]Illingworth, C. R., "Steady Flow in the Laminar Boundary Layer of a Gas," *Proceedings of the Royal Society (London), Series A*, Vol. 199, No. 1059, 1949, pp. 533–558.

[21]Stewartson, K., "Correlated Incompressible and Compressible Boundary Layers," *Proceedings of the Royal Society (London), Series A*, Vol. 200, No. 106, 1949, pp. 84–100.

[22]Howarth, L., "Concerning the Effect of Compressibility on Laminar Boundary Layers and Their Separation," *Proceedings of the Royal Society (London), Series A*, Vol. 194, No. 1036, 1948, pp. 16–42.

[23]Dorodnitsyn, A. A., "Laminar Boundary Layer in Compressible Fluid," *Doklady Akademii Nauk SSSR*, Vol. 34, 1942, pp. 213–219.

[24]Anderson, J. D., *Hypersonic and High Temperature Gas Dynamics*, McGraw–Hill, 1989, pp. 219–250.

[25]White, F. M., *Viscous Fluid Flow*, McGraw–Hill, New York, 1991, p. 246.

[26]Davis, R. T., Merle, M. J., and Polak, A., *Introduction to Boundary-Layer Theory*, Dept. of Aerospace Engineering and Applied Mechanics, Univ. of Cincinnati, Cincinnati, OH, Dec. 1980.

[27]Tannehill, J. C., Anderson, D. A., and Pletcher, R. H., *Computational Fluid Mechanics and Heat Transfer*, Taylor and Francis, Philadelphia, 1997, p. 454.

[28]Blottner, F. G., "Investigation of Some Finite-Difference Techniques for Solving the Boundary Layer Equations," *Computer Methods in Applied Mechanics and Engineering*, Vol. 6, No. 1, 1975, pp. 1–30.

[29]Hamilton, H. H., Millman, D. R., and Greendyke, R. B., "Finite-Difference Solution for Laminar or Turbulent Boundary Layer Flow over Axisymmetric Bodies with Ideal Gas, CF_4, or Equilibrium Air Chemistry," NASA TP-3271, Dec. 1992.

A. Plotkin
Associate Editor